

**EFFECT OF ERBIUM-CALCIUM MANGANITE DOPING ON MICROSTRUCTURE  
AND ELECTRICAL PROPERTIES OF ZINC OXIDE BASED VARISTOR  
CERAMICS**

M. A. Zulkifli<sup>1</sup>, M. S. M. Ghazali<sup>1</sup>, W. R. W. Abdullah<sup>2</sup>, A. Zakaria<sup>3</sup>, Z. Ahmad<sup>1</sup> and R. Umar<sup>4,\*</sup>

<sup>1</sup>School of Fundamental Science, Universiti Malaysia Terengganu, 21030 Kuala Terengganu, Terengganu, Malaysia

<sup>2</sup>School of Ocean Engineering, Universiti Malaysia Terengganu, 21030 Kuala Terengganu, Terengganu, Malaysia

<sup>3</sup>Department of Physics, Faculty of Science, Universiti Putra Malaysia, 43400 Serdang, Selangor, Malaysia

<sup>4</sup>East Coast Environmental Research Institute (ESERI), University Sultan Zainal Abidin, Gong Badak Campus, 21300 Kuala Terengganu, Terengganu, Malaysia

Published online: 08 August 2017

---

**ABSTRACT**

In this research, (80-x) mol% zinc oxide with 20 mol% CaMnO<sub>3</sub> as the additive and (x) mol% erbium oxide Er<sub>2</sub>O<sub>3</sub> as the doping material where x = 0.5, 1.0 and 1.5. Aims of this work are to elucidate the effects of doping material on microstructure ZnO and nonlinear characteristics of ZnO based varistor ceramics. A compound comprising ZnO-CaMnO<sub>3</sub>-Er<sub>2</sub>O<sub>3</sub> underwent pre-sintering at 500 °C for 4 hours and sintering process at temperature of 1100 °C, 1200 °C and 1300 °C with the soaking time of 1.5 hours and 4.5 hours. X-ray diffraction patterns confirmed the presence of CaMnO<sub>3</sub> spinal and additional phases containing Er in the synthesized compounds.

---

Author Correspondence, e-mail: [mohdsabri@umt.edu.my](mailto:mohdsabri@umt.edu.my)

doi: <http://dx.doi.org/10.4314/jfas.v9i2s.20>



The disappeared of hydroxyl and carbonyl functional group was observed at 3600-3650  $\text{cm}^{-1}$ , 1421  $\text{cm}^{-1}$  and 875  $\text{cm}^{-1}$  respectively by Fourier Transform Infrared spectroscopy to indicate the starting formation oxide metal upon calcinations.

**Keywords:** ZnO varistor; Er doping; microstructure; I-V characteristics; low voltage varistor.

## 1. INTRODUCTION

Varistor also known as voltage dependent resistor (VDR) widely use as over voltage protection. Varistor operate by literally absorbing the dangerous surge and spikes or grounding its. Overvoltage protection is a necessity for electronic circuits, in the electrical power distribution and transmission industries [1-3]. Zinc oxide (ZnO) as a based varistor commonly study due to its capability and good performance. The electrical characteristics of ZnO based varistor are similar to diodes, varistors can limit overvoltage equally in both polarities therefore the current-voltage characteristics of a varistor, which is analogous to that of two back-to-back diodes, can increase significantly. Varistors can be operated in either alternative or direct current with the fields ranging from a few volts to tens of kilovolts per metre and a wide range of current as well.

Usually, metal oxide as additive materials introduce to ZnO based varistor are  $\text{Bi}_2\text{O}_3$ ,  $\text{MnO}_2$  and  $\text{Co}_3\text{O}_4$  [5-6]. Among metal oxide used,  $\text{Bi}_2\text{O}_3$  most frequently used. However, with concern to produced low voltage varistor,  $\text{Pr}_6\text{O}_{11}$  start to study as alternative additive to produced low voltage varistor. Used of  $\text{Pr}_6\text{O}_{11}$  as answer to high volatility and reactivity in  $\text{Bi}_2\text{O}_3$  [5, 7-8]. Extensive study by [9] with introduced  $\text{CaMnO}_3$  shows capability of perovskite structure onto low voltage application.

In this study, the effects of  $\text{Er}_2\text{O}_3$  mol%, sintering process (soaking temperature and time) on microstructure and electrical characteristics of  $(\text{CaMnO}_3\text{-Er}_2\text{O}_3)$ -doped zinc oxide varistor ceramics were systematically investigated and new results were attained.

## 2. RESULTS AND DISCUSSION

### 2.1. Synthesis of ZnO-CaMnO<sub>3</sub>-Er<sub>2</sub>O<sub>3</sub>

XRD analysis shows the phase change from citrate complexes phase to crystallite form for

drying to calcine stages. At the calcine stage, major ZnO peaks identified. While at the sintered stage, disappear peaks of perovskite structures manganocalcite  $(\text{Ca},\text{Mn})\text{CO}_3$  at  $29^\circ$  (030) clearly observed and identified in this work. This identification shows good agreement with our previous reported study [10]. Minor peaks of  $\text{Er}_2\text{O}_3$  and  $\text{CaMnO}_3$  also appeared after sintering process.

FTIR analysis also indicated the same phenomena, where from the complexes bonding (drying stage) turn to carbonate bonding ( $-\text{CO}_3$ ) by calcination proses. Completed formation metal oxide was a observed in sintered graph by disappeared of  $-\text{CO}_3$  at peak 1433, 112 and 113  $\text{cm}^{-1}$  [7, 10]. Thus, by the XRD (Fig. 1) and FTIR (Fig. 2), both proved the transformation from complexes phase/bonding (dried stage) to crystallite phase and formation  $-\text{CO}_3$  (calcined stage), further turn to highly crystallite and formation metal oxide bonding (sintered stage).

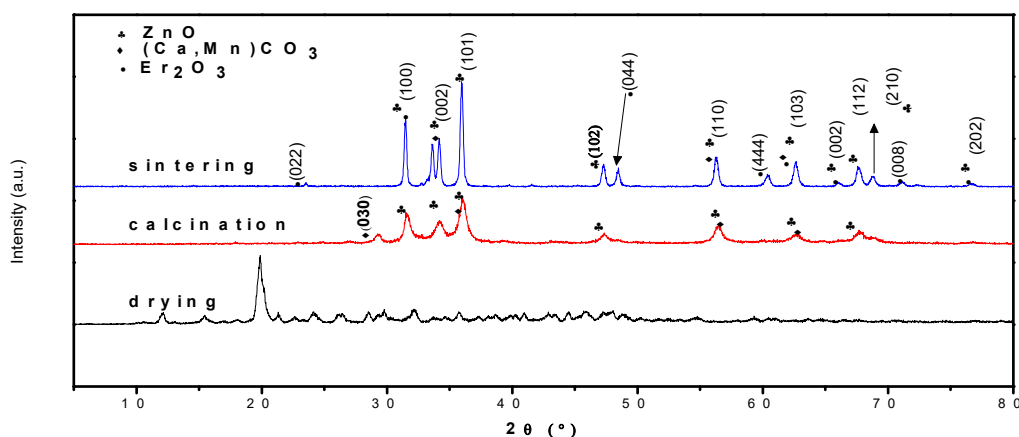


**Fig.1.** XRD patterns of different type of heat treatment

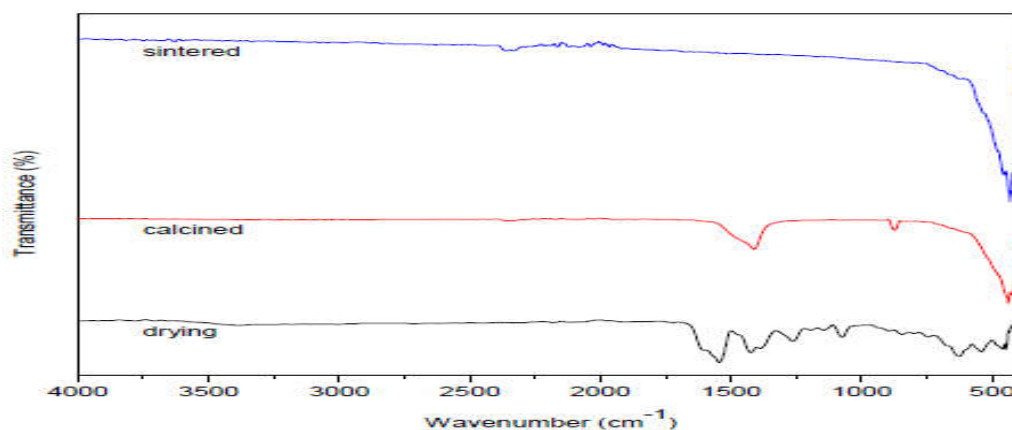


**Fig.2.** FTIR of  $(\text{ZnO}-\text{CaMnO}_3-\text{Er}_2\text{O}_3)$  compound undergoes dried, calcined and sintered process

EDS analysis further confirm the elements and compounds present in each systems (Table 1-3). Mass % of  $\text{Er}_2\text{O}_3$  is directly proportional with the increases of  $\text{Er}_2\text{O}_3$  mol% in systems. This increases also indicated by appearance of  $\text{Er}_2\text{O}_3$  peak at 76.64 degree with the intensity of 0.5 mol%  $\text{Er}_2\text{O}_3$  (38.33), 1.0 mol%  $\text{Er}_2\text{O}_3$  (1054.00) and 1.5 mol%  $\text{Er}_2\text{O}_3$  (2371.33) on XRD graph (Fig. 3).

**Table 1.** The mass% of 0.5 mol% in  $\text{Er}_2\text{O}_3$  by EDS

Element	(keV)	mass%	Error%	At%	Compound	mass%	Cation	K
O		20.73						
Ca K	3.69	5.51	0.16	10.66	CaO	7.71	2.55	7.9403
Mn K	5.894	12.26	0.28	17.3	MnO	15.83	4.13	15.946
Zn K	8.63	60.56	0.76	71.83	ZnO	75.38	17.16	75.088
Er L	6.943	0.95	0.92	0.22	$\text{Er}_2\text{O}_3$	1.09	0.11	1.0241
Total		100		100		100	23.95	

**Table 2.** The mass% of 1.0 mol% in  $\text{Er}_2\text{O}_3$  by EDS

Element	(keV)	mass%	Error%	At%	Compound	mass%	Cation	K
O		20.43						
Ca K	3.69	4.23	0.19	8.3	CaO	5.91	1.98	6.0351
Mn K	5.894	8.61	0.34	12.33	MnO	11.12	2.95	11.247
Zn K	8.63	65.76	0.92	79.14	ZnO	81.85	18.91	81.642
Er L	6.943	0.98	1.1	0.23	$\text{Er}_2\text{O}_3$	1.12	0.11	1.0721
Total		100		100		100	23.94	

**Table 3.** The mass% of 1.5 mol% in  $\text{Er}_2\text{O}_3$  by EDS

Element	(keV)	mass%	Error%	At%	Compound	mass%	Cation	K
O		20.61						
Ca K	3.69	5.99	0.12	11.76	CaO	8.38	2.78	8.6211
Mn K	5.894	11.77	0.22	16.85	MnO	15.2	3.99	15.332
Zn K	8.63	58.76	0.59	70.71	ZnO	73.14	16.74	72.951
Er L	6.943	2.87	0.72	0.67	$\text{Er}_2\text{O}_3$	3.28	0.32	3.0936
Total		100		100		100	23.84	

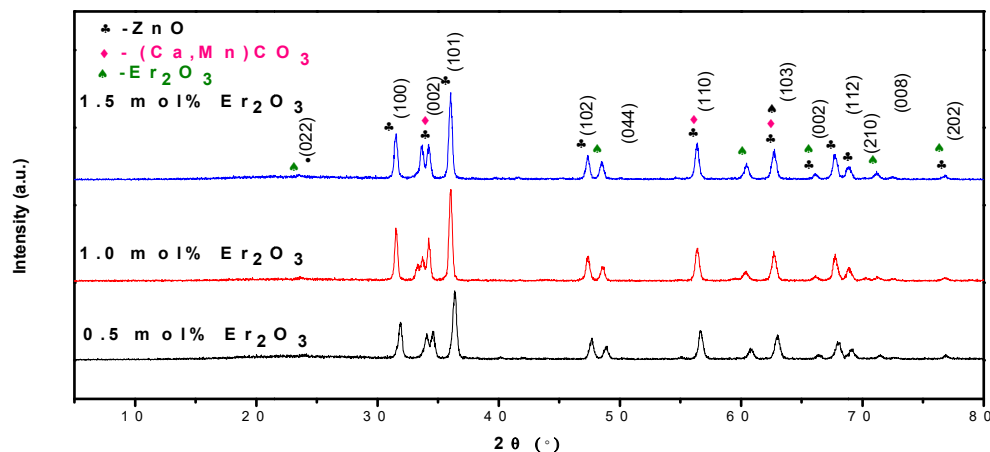


Fig.3. Different molarities of  $\text{Er}_2\text{O}_3$  in precursor powder

### 3.2. Microstructures analysis of $\text{ZnO-CaMnO}_3\text{-Er}_2\text{O}_3$

Microstructure characteristics of  $\text{ZnO-CaMnO}_3\text{-Er}_2\text{O}_3$  were altered by the effect of mol%  $\text{Er}_2\text{O}_3$  dopant with sintering temperatures (1100, 1200 and 1300 °C) and soaking times (1.5 hour and 4.5 hour). SEM images (Fig. 4) shows the porosity phenomena occur in all samples. However, the distributions of porosity are different. The increased of porosity in pellet surface and it believe causes by the increased of concentration of  $\text{Er}_2\text{O}_3$  dopant. This behaviour was affected by limited substitution of  $\text{Er}^{+3}$  ion into  $\text{ZnO}$  grains. This limited substitution occurs as consequence of larger radius size of  $\text{Er}^{+3}$  ion (0.088 nm) compared to  $\text{Zn}^{+2}$  ion. By the different ions radius size creates the lattice defect in  $\text{ZnO}$  grains that obviously observed by porosity [11].

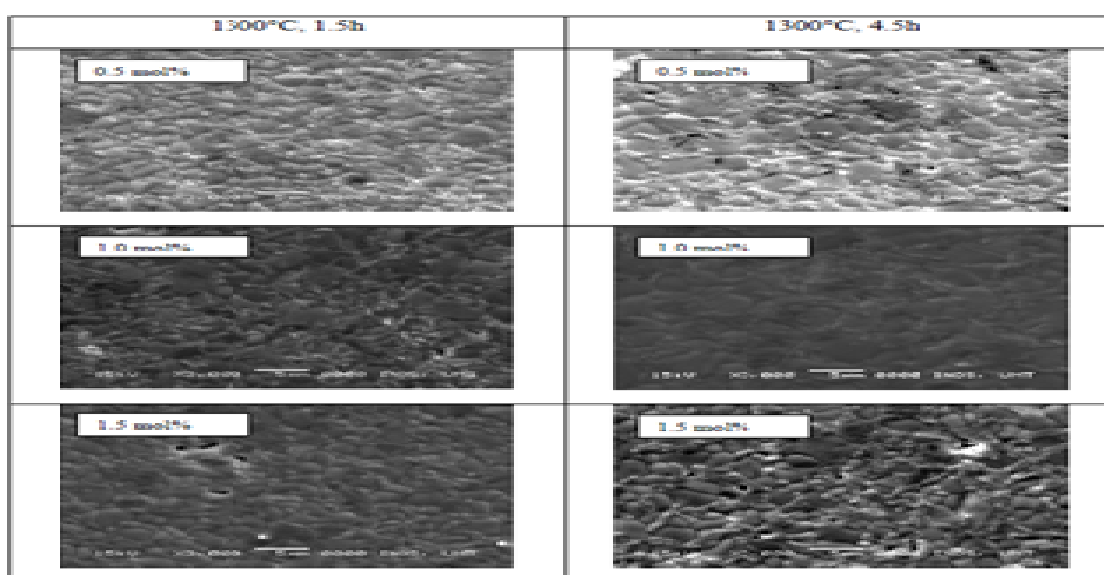


Fig.4. SEM images of the samples sintered at different molarities of  $\text{Er}_2\text{O}_3$

Table 4 represented the density ( $\rho$ ) and average grain size that effected by sintering temperatures and soaking time. The  $\rho$  value increased with the increased of soaking time. While, the average grains size further increase with the increases of sintering temperatures and soaking times. A same pattern was reported by [12-13]. Distribution of grains sizes was attributing by the separation of Er toward grain boundaries causes the different in ionic radius [11]. Thus, the consideration of sintering temperature is an importance driving force for the grain growth [12].

**Table 4.** The comparison of density and average grain size with sintering temperature and time

Sintering		$\rho$ , (g/cm <sup>3</sup> )	Average grain size, ( $\mu$ m)
T, (°C)	Time, (h)		
1100	1.5	5.5627	1.28
	4.5	5.8144	1.60
1200	1.5	5.3437	1.42
	4.5	5.4094	2.71
1300	1.5	6.0746	2.77
	4.5	5.9084	3.00

### 3.3. Electrical characteristics of ZnO-CaMnO<sub>3</sub> Er<sub>2</sub>O<sub>3</sub>

Value of  $\alpha$  was measured based on J-E plotted graph. The  $\alpha$  value measured in range of 1-10 mA. Summary of leakage current density (JL) and electrical field (Eb) was tabulated on Table 5. The  $\alpha$  value were affected by the mol% Er<sub>2</sub>O<sub>3</sub> dopant, sintering temperatures and soaking times. Generally, the  $\alpha$  increase with the increase of sintering temperature from 1100 to 1200 °C. It is due to increase of grains size and decrease of grain boundaries. However, the value of  $\alpha$  while the sintering temperature up to 1300 °C. This behavior was affected by the increase of porosity on varistor ceramics microstructure. The JL value was directly

proportional with the Eb.

**Table 5.** The results of JL, Eb and  $\alpha$

T (°C)	Er <sub>2</sub> O <sub>3</sub> (mol %)	Time (Hrs)	J <sub>1</sub> (A/cm <sup>2</sup> ) (± 0.05-0.10)	E <sub>b</sub> (V/cm) (± 0.05-0.10)	$\alpha$ (± 0.05-0.10)
1100	0.5	1.5	0.352	0.44	1.6168
		4.5	4.857144	6.07143	2.42464
	1.0	1.5	4.853336	6.06667	1.74768
		4.5	18.27027	22.83784	2.04213
	1.5	1.5	2.349208	2.93651	1.6668
		4.5	2.244896	2.80612	2.42464
1200	0.5	1.5	3.744	4.68	2.25601
		4.5	2.464	3.08	3.79827
	1.0	1.5	7.69652	9.62065	2.48198
		4.5	3.63636	4.54848	2.0038
	1.5	1.5	2	2.5	1.74768
		4.5	3.009904	3.76238	2.04213
1300	0.5	1.5	0.537312	0.67164	1.52629
		4.5	0.885496	1.10687	1.83468
	1.0	1.5	12.74074	15.92593	1.50103
		4.5	0.431656	0.53957	2.81158
	1.5	1.5	3.208336	4.01042	2.11491
		4.5	1.872344	2.34043	2.82860

### 3. EXPERIMENTAL

#### 3.1. Materials

Raw materials were prepared according to the composition of (100-20.0-x) mol% ZnO + 20.0 mol% CaMnO<sub>3</sub> + x mol% Er<sub>2</sub>O<sub>3</sub> (x = 0.5, 1.0 and 1.5). Reagent Calcium acetate monohydrate with the purity of 99.0% (Sigma Aldrich), Manganese (II) acetate-4-hydrate (Hamburg Chemical) and Erbium (III) acetate hydrate (Sigma Aldrich) was used as metal salt precursor and citric acid anhydrous (C<sub>2</sub>H<sub>6</sub>O<sub>8</sub>) with the purity of 99.5% (Alfa Aesar) was selected as the complexing agent. ZnO powder with the particle size of less than 1  $\mu$ m and 99.9% purity (Sigma Aldrich) was selected as the host material.

#### 3.2. Sample Preparation

Fully coating of Ca-Mn-Er citrate gel with ZnO particles was produced by adding ZnO powder into bath solution that comprising Ca-Mn-Er acetate and citric acid in medium of deionized water. This gel moisture were continues stir for 1 hour retention time at 60 to 80 °C. The molar ratio of calcium acetate/manganese (II) acetate/ erbium (III) acetate to citric acid anhydrous was fixed at 1:2 and vigorous stirring was applied to improve the contact. Uniform coating of Ca-Mn-Er citrate gel with ZnO particles was produced by immersing ZnO powder in bath solution containing citric acid and Ca-Mn-Er acetate in deionized water medium for 1

hour retention time at 70-80 °C. Then, this mixtures dried at 120 °C for 19 h to produce powder with particle size of less than 100 µm. After drying the powder slurry, the mixture powder was then calcined at 500 °C for 4 h at heating rate of 3 °C/min. The calcined powder comprising 1.75 wt.% polyvinyl alcohol binder was granulated using a sieving shaker with 68µ-mesh screen and pressed into disk shaped pellets of 10 mm in diameter and ≈1.5 mm in thickness at a pressure of 2.6 T using Specac Hydraulic Press machine. The pellet was finally sintered at 1100, 1200 and 1300 °C for 1.5 and 4.5 h in a box furnace.

### 3.3. Characterizations

#### 3.3.1. Surface Morphology and Microstructure Analysis

The polycrystalline, phase changing and spinel phases were identified by an X-ray diffractometer (XRD) by using Rigaku Mini Flex II Diffractometer with CuK $\alpha$  radiation. A small amount sample was spread uniformly and homogenously on the XRD's sample holder, 2 $\theta$  scan were carried out over the diffraction angles from 5° to 80° at the speed of 2.00°min<sup>-1</sup>. Appearing and disappearing important functional group of compound elements during drying, calcined and sintering process were identified using IRTracer- 100 Fourier Transform Infrared (FTIR) Spectrophotometer (Brand: SHIMADZU) with starting wavelength of 450 cm<sup>-1</sup> until 4000 cm<sup>-1</sup>. The densities ( $\rho$ ) of sintered pellets were measured by using an electronic Densimeter (Model MDS-300) (Resolution 0.001). The  $\rho$  measurement value is important to illustrate the porosity on sintered pellets.

Scanning electron microscope (SEM) attached with energy dispersive spectroscopy (EDS) (Model JEOL JSM-6360LA) were used to observe the surface morphology, and then measure their grains size and to identify the present of elements on sintered pellets respectively.

#### 3.3.2. Electrical Characteristics Measurement

Electrical characteristics of sintered pelleted sample was measured by using a 4200-SCS Semiconductor Characterization System, Brand Keithley. 15 wt% and silver conductive paint were placed on the both side of the samples as an electrodes. The nonlinear coefficient ( $\alpha$ ) was determined from the Equation (1)

$$\alpha = \frac{\log(I_2 / I_1)}{\log(V_2 / V_1)} \quad (1)$$

#### 4. CONCLUSION

As conclusions, ZnO-CaMnO<sub>3</sub>-Er<sub>2</sub>O<sub>3</sub> varistor ceramic was successful produced in low voltage behavior. XRD patterns confirmed the presence of CaMnO<sub>3</sub> spinel and additional phases containing Er in the synthesized compounds. The disappeared of hydroxyl and carbonyl functional group was observed at 3600-3650 cm<sup>-1</sup>, 1421 cm<sup>-1</sup> and 875 cm<sup>-1</sup> respectively by Fourier Transform Infrared (FTIR) spectroscopy to indicate the starting formation oxide metal upon calcinations. EDS measurement furthers confirm mass % of Er<sub>2</sub>O<sub>3</sub> with supportive intensity peak on XRD result. Electrical properties of ZnO-CaMnO<sub>3</sub>-Er<sub>2</sub>O<sub>3</sub> were measured by leakage current density, electrical field and nonlinear coefficient. Current-voltage (I-V) characteristics showed the value of nonlinear coefficient in the range of 1.0 to 4.0. Effects of Er doping observed by altered on grains microstructure of ZnO varistor ceramics and electrical properties parameters changing.

#### 5. ACKNOWLEDGEMENTS

The authors would like to acknowledge the Ministry of Higher Education Malaysia for providing fund for this research under Research Acculturation Grant Scheme (RAGS) (Vot No. 57114) and laboratory of Physics, Universiti Malaysia Terengganu.

#### 6. REFERENCES

- [1] Ellmer K, Klein A. ZnO and its applications. In K. Ellmer, A. Klein, & B. Rech (Eds.), Transparent conductive zinc oxide. Berlin: Springer-Verlag, 2008, pp.1-33
- [2] Gupta T K. Application of zinc oxide varistors. Journal of the American Ceramic Society, 1990, 73(7):1817-1840
- [3] Ivon A I, Glot A B, Lavrov R I, Bubel T A. Temperature dependence of zinc oxide grain resistivity in ZnO varistor ceramics. Journal of Alloys and Compounds, 2016, 656:740-744
- [4] Matsuoka M. Nonohmic properties of zinc oxide ceramics. Japanese Journal of Applied Physics, 1971, 10(6):736-746
- [5] Wang M H, Zhao Z Y, Liu T T. Synthesis of Pr-doped ZnO nanoparticles by sol-gel method and varistor properties study. Journal of Alloys and Compounds, 2015, 621:220-224

- [6] Dong X U, Shi X F, Cheng X N, Juan Y A, Fan Y E, Yuan H M, Shi L Y. Microstructure and electrical properties of Lu<sub>2</sub>O<sub>3</sub>-doped ZnO-Bi<sub>2</sub>O<sub>3</sub>-based varistor ceramics. Transactions of Nonferrous Metals Society of China, 2010, 20(12):2303-2308
- [7] Wan Abdullah W R, Zakaria A, Ghazali M S. Synthesis mechanism of low-voltage praseodymium oxide doped zinc oxide varistor ceramics prepared through modified citrate gel coating. International Journal of Molecular Sciences, 2012, 13(4):5278-5289
- [8] Wang Q, Qin Y, Xu G J, Chen L, Li Y, Duan L, Li Z X, Li Y L, Cui P. Low voltage ZnO varistor fabricated by the solution coating method. Ceramics International, 2008, 34(7):1697-1701
- [9] Vijayanand Vijayanandhini K, Kutty T R. Calcium zinc manganites, Ca<sub>4</sub>Mn<sub>7</sub>Zn<sub>3</sub>O<sub>21-δ</sub> (0.5 < δ < 2.5) with beta-alumina or magnetoplumbite-type structure and their nonlinear electrical transport and magnetic properties. Materials Letters, 2007, 61(17):3652-3657
- [10] Zulkifli M A, Ghazali M S, Abdullah W R, Zakaria A, Ahmad Z. Preliminary characteristic of electrical non-linearity Co doped CaMnO<sub>3</sub>-ZnO based varistor ceramics. Jurnal Teknologi, 2016, 78(3):327-U312
- [11] Nahm C W, Park C H. Effect of Er<sub>2</sub>O<sub>3</sub> addition on the microstructure, electrical properties, and stability of Pr<sub>6</sub>O<sub>11</sub>-based ZnO ceramic varistors. Journal of Materials Science, 2001, 36(7):1671-1679
- [12] Choon W N. Sintering effect on electrical properties and pulse aging behavior of (V<sub>2</sub>O<sub>5</sub>-Mn<sub>3</sub>O<sub>4</sub>-Er<sub>2</sub>O<sub>3</sub>)-doped zinc oxide varistor ceramics. Journal of Rare Earths, 2014, 32(1):29-36
- [13] Choon W N. Effect of erbium on varistor characteristics of vanadium oxide-doped zinc oxide ceramics. Journal of Materials Science: Materials in Electronics, 2012, 24(1):27-35

**How to cite this article:**

Zulkifli MA, Ghazali MSM, Abdullah WRW, Zakaria A, Ahmad Z, Umar R. Effect of erbium-calcium manganite doping on microstructure and electrical properties of zinc oxide based varistor ceramics. J. Fundam. Appl. Sci., 2017, 9(2S), 298-307.